Oxygen plasma treatment WO_3 nanorods for Improvement H_2S gas sensing

Chaiyan Oros[a,*], Phusit Sangpradub[b], Preeyanut Daunglaor[b], Thita Yodsawad[b]

[a] Faculty of Science and Technology, Rajamangala University of Technology Rattanakosin, Nakornpathom, 73170 Thailand
[b] Faculty of Liberal-Arts, Rajamangala University of Technology Rattanakosin, Nakornpathom, 73170 Thailand

***Corresponding Author:** chaiyan.oro@rmutr.ac.th
https://doi.org/10.55674/jmsae.v13i2.248329

Received: 29 April 2022 | **Revised:** 18 June 2022 | **Accepted:** 05 February 2024 | **Available online:** 1 May 2024

Abstract

Herein, the oxygen (O_2) plasma has been used to post-treat tungsten oxide (WO_3) nanorods to improve the sensing performance of the H_2S gas sensor. The reactive DC magnetron sputtering process with the glancing-angle deposition (GLAD) technique was used to prepare the WO_3 nanorods. After deposition, the WO_3 nanorod thin films were treated with O_2 plasma at different treatment power from 100 – 200 W. The physical structure of as-deposition and treated WO_3 nanorod thin films was investigated crystal structure and morphology by grazing incident X-ray diffraction (GIXRD), field-emission scanning electron microscope (FE-SEM), and high-resolution transmission electron microscope (HRTEM). The result indicated that the WO_3 nanorod structure transformed to the monoclinic polycrystalline phase. FE-SEM and HRTEM observed slight changes in the shape of the WO_3 nanorods. The H_2S sensing properties were measured at 10 ppm at 150 – 350°C operating temperatures. At an operating temperature of 200 °C, the response to H_2S of O_2 plasma treated WO_3 nanorods is increased by a factor of 5 – 15, and the maximum response to H_2S is 15. The results showed that the O_2 plasma treatment process improved the sensing response of the WO3 nanorods.

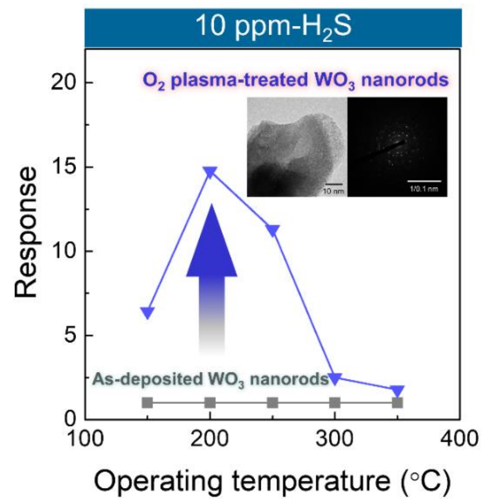

Keywords: WO_3 nanorods; Oxygen plasma; H_2S sensor; GLAD technique

Introduction

Tungsten Oxide (WO_3) is an n-type semiconductor and has an energy gap of approximately 2.60 – 3.60 eV, which can be applied in many technologies such as electrochromic, photocatalytic, photovoltaic, and gas-sensor technology. For the gas-sensor technology, the semiconductor gas sensing of WO_3 has been widely studied since it has high sensitivity, high stability, and fast response to many gases such as ethanol, NO_2, H_2, and H_2S [1 – 3]. Moreover, WO_3 can be fabricated into many nanostructure patterns, such as nanotubes, nanowires, nanorods, etc. The WO_3 nanostructured gas sensors were effective for high sensitivity and fast response due to their large surface area and optimum crystallinity [4 – 6]. Increasing the surface area and crystallization by plasma treatment is an interesting technique [7]. Several processes were used to synthesize WO_3 nanostructures, such as physical vapor deposition (PVD), chemical vapor deposition (CVD), thermal oxidization, flame spray pyrolysis, and hydrothermal [8 –10]. However, there are many processes to prepare WO_3 nanostructures that cannot control their sizes, distributions, formation, and reproducibility. Therefore, a physical vapor deposition (PVD) method with the GLAD technique is most suitable for synthesizing WO_3 nanostructures [11, 12]. The GLAD technique is an oblique angle deposition (OAD) method with substrate rotation to synthesize a columnar nanorod structure. The porosity and shape of the nanorod structure can be controlled by the self-shadowing effect and surface diffusion of the initial nucleation island during the deposition process [13 – 15].

Materials and Methods

The WO_3 nanorods were synthesized, and the O_2 plasma treatment was processed by a reactive DC magnetron sputtering system with the GLAD technique, as shown in the symmetric diagram in Fig. 1. The silicon wafers (100) were used as substrates for physical property analysis, and an ultrasonic washer cleaned them in acetone. Then, the SiO_2/Si with interdigitated gold electrodes were used as substrates for H_2S gas sensor testing. For the sputtering process, the sputtering target was a metallic tungsten disc, and the substrate was 7 cm from the target. Then, the substrate was installed at an angle with the vapor incident flux equal to 85° and the substrate rotation speed fixed at 5 rpm. The WO_3 nanorods are prepared under the atmosphere with argon (Ar) and O_2 flow rates of 12 and 48 sccm, respectively. The base pressure and operated pressure are 6×10^{-6} and 5×10^{-3} mbar, respectively. The deposition time was fixed at 90 min. After growth, the WO_3 nanorod samples were treated with the O_2 plasma at different power from 100 – 200 W for 10 min. The crystal structures of the WO_3 nanorods were analyzed by the GIXRD technique, obtained from a grazing incident X-ray diffractometer operating with an incident angle of 20° – 60°. The morphology of the WO_3 nanorods was analyzed by a field-emission scanning electron microscope (FE-SEM) and a high-resolution transmission electron microscope (HRTEM). For H_2S gas sensor testing, the tungsten oxide nanorods were deposited on interdigitated electrodes and mounted in a gas-testingchamber. The purified air and H_2S gas were mixed with the concentration of H_2S gas at 10 ppm and made to flow through the testing chamber. Then, the H_2S gas sensor was tested with an operating temperature varied from 150 – 350 °C and heated by an external heater.

Results and Discussions

The GIXRD pattern of as-deposited and O_2 plasma-treated WO_3 nanorods is shown in Fig. 2. It can be found that the as-deposited and plasma-treated WO_3 nanorods at 100 –150 W exhibit an amorphous structure. When the O_2 plasma treatment is increased to 200 W, the polycrystalline structure of the WO_3 monoclinic phase can be observed. This might be because the plasma treatment could enhance the internal heating of the sample during the treatment process. Generally, the crystalline transition from amorphous to polycrystalline WO_3 occurs when the samples are annealed at 300 – 400 C° [15].

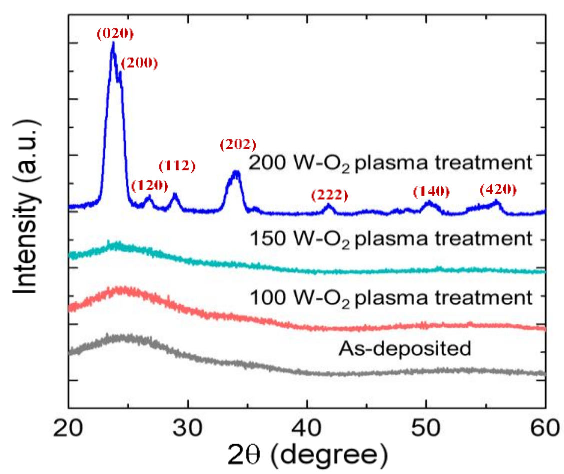

Fig. 2 GIXRD patterns of as-deposited and oxygen plasma-treated WO_3 nanorods.

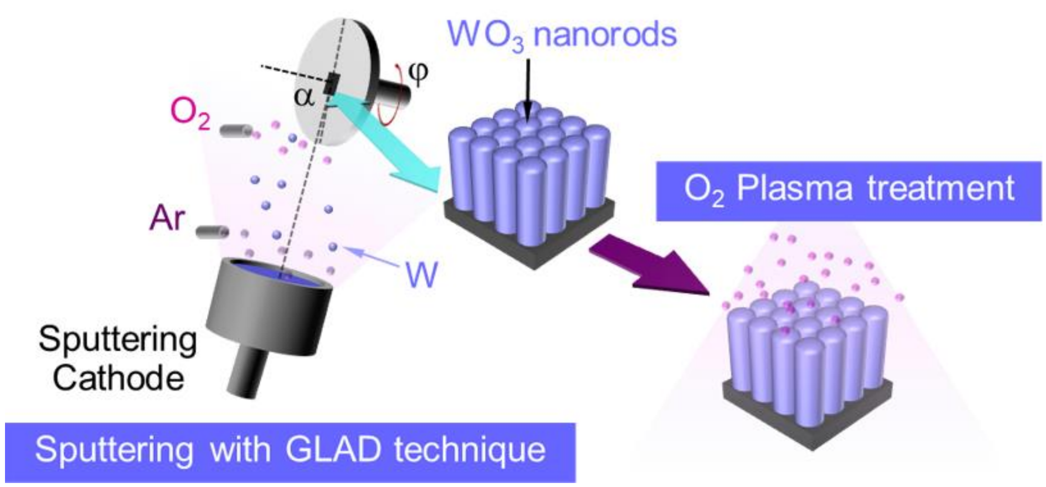

Fig. 1 Schematic diagram of the GLAD technique and O_2 plasma treatment process.

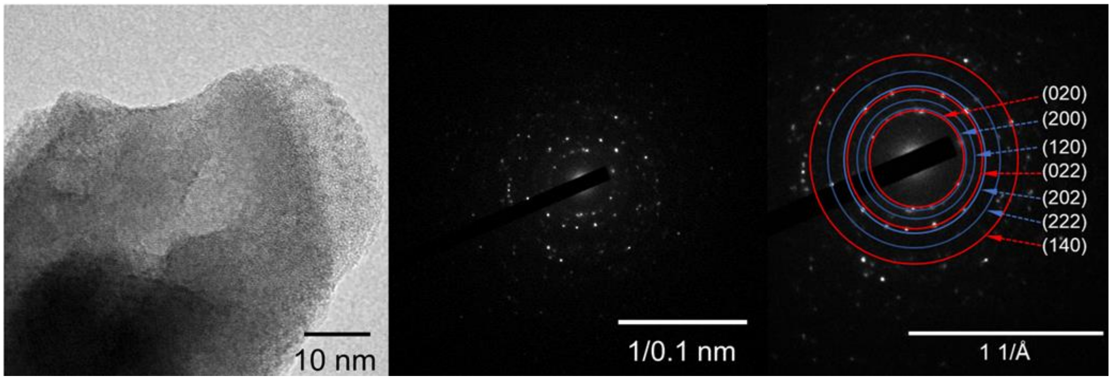

Fig. 3 HRTEM image of 200 W-O_2 plasma-treated WO_3 nanorods.

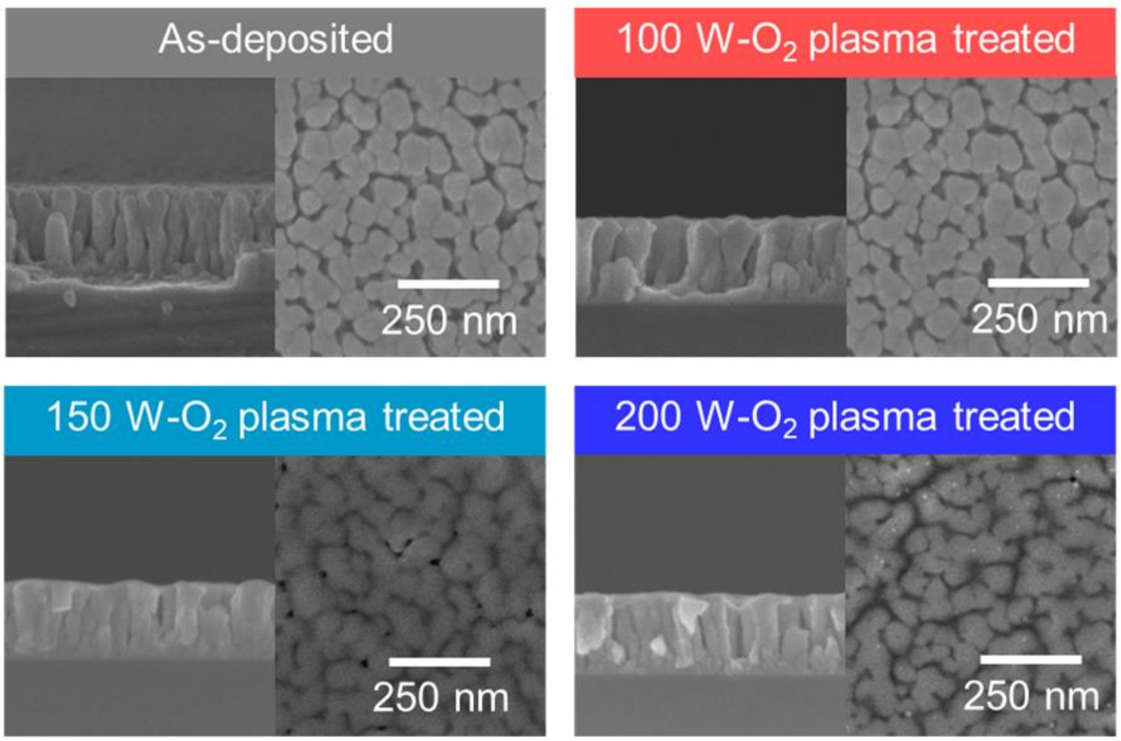

Fig. 4 FE-SEM images of as-deposited and oxygen plasma-treated WO_3 nanorods.

Fig. 3 shows the typical HRTEM and selected area diffraction electron (SADE) images from the tip of the O_2 plasma-treated WO_3 nanorods at 200 W. The crystalline structure of the WO_3 nanorods was clearly observed in the HRTEM image. In addition, the SADE pattern indicates that the plasma-treated WO_3 nanorods at 200 W were polycrystalline, which corresponds to the GIXRD result in the previous section.

The FE-SEM images of as-deposited and O_2 plasma-treated WO_3 nanorods are shown in Fig. 4. The results indicate that all the thin films of tungsten oxide nanorods show columnar nanorod structures. The average diameter of WO_3 nanorods is estimated to be 60 nm, and the WO_3 nanorods thickness of as-deposited and O_2 plasma-treated WO_3 nanorods at 100, 150, and 200 W were measured to be approximately 233, 200, 267 and 150 nm, respectively, as shown in Fig. 5. However, the surface morphology of the plasma-treated WO_3 nanorods at high power showed a smooth surface. In addition, the thickness of the WO_3 nanorod layer decreased with the increase in O_2 plasma treatment power. The decrease in the smooth surface and etching thickness layer might be due to the O_2 interaction with the nanorod surface, which indicates that the energy of the O_2 plasma plays a major role in morphology control.

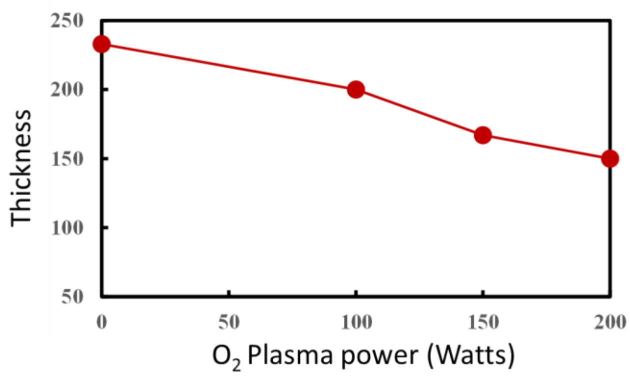

Fig. 5 WO_3 nanorods thickness of as-deposited and O_2 plasma-treated at 100, 150 and 200 W.

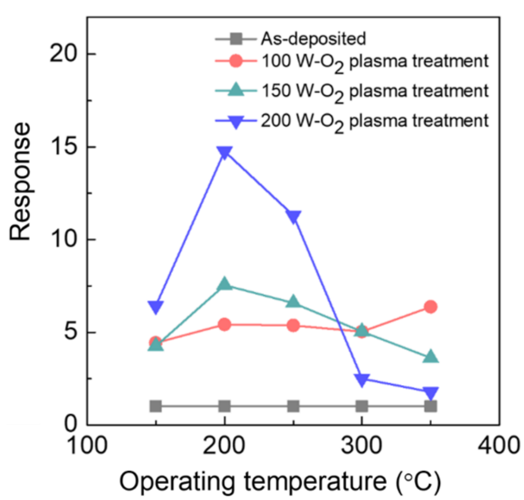

Fig. 6 H_2S gas response of as-deposited and oxygen plasma-treated WO_3 nanorods.

As shown in Fig. 6, as-deposited and O_2 plasma-treated WO_3 nanorods were measured toward 10 ppm-H_2S gas at operating temperatures ranging from 150 – 350 °C. The as-deposited WO_3 nanorods showed an inadequate response. It can be found that the H_2S gas responses of plasma-treated WO_3 nanorods increase as the operating temperature increases from 150 – 200 °C. The response to H_2S of O_2 plasma treatment WO_3 nanorods is increased by about a factor of 5 – 15 depending on temperature and the adsorbed surface oxygen species. In addition, the O_2 plasma treatment of WO_3 nanorods exhibits a maximized response to H_2S of 15 at an operating temperature of 200 °C. The experimental results indicate that O_2 plasma treatment significantly enhances the H_2S sensing performance by a 380% improvement compared to a dense WO_3 film. This improvement can be attributed to the modifications in the structure and the increased surface area achieved through the O_2 plasma treatment [17 – 20].

Conclusion

In conclusion, we present the crystal structure, morphology, and H_2S sensing of as-deposited and oxygen plasma-treated WO_3 nanorods on Si substrate. The post-O_2 plasma treatment at 200 W promoted the polycrystalline WO_3 nanorods. The plasma-treated WO_3 nanorods at high O_2 plasma power tend to smooth surface and decrease in thickness. In addition, the plasma-treated WO_3 nanorods at 200 W were revealed to be promising for achieving H_2S sensors with a high response of about 15 at 200 °C optimum operating temperature compared with as-deposited WO_3 nanorods.

Acknowledgements

This work has financial support from Rajamangala University of Technology Rattanakosin, and the author is thankful to the Opto-Electrochemical Sensing Research Team, National Electronics and Computer Technology Center, Thailand, for the preparation and characterization system.

References

[1] Y. Shen, T. Yamazaki, Z. Liu, D. Meng, T. Kikuta, N. Nakatani, Influence of Effective Surface Area on Gas Sensing Properties of WO_3 Sputtered Thin Films, Thin Solid Films. 517 (2009) 2069 – 2072.

[2] D. Deniz, D.J. Frankel, R.J. Lad, Nanostructured tungsten and tungsten trioxide films prepared by glancing angle deposition, Thin Solid Films. 518 (2010) 4095 – 4099.

[3] M. Horprathuma, K. Limwicheana, A. Wisitsoraat, P. Eiamchai, K. Aiempanakit, P. Limnonthakul, N. Nuntawong, V. Pattantsetakul, A. Tuantranont, P. Chindaudom, NO_2-sensing properties of WO_3

nanorods prepared by glancing angle DC magnetron sputtering, Sens. Actuators B Chem. 176 (2013) 685 – 691.

[4] Y.B. Li, Y. Bando, D. Golberg, K. Kurashima, WO_3 Nanorods/Nanobelts Synthesized via Physical Vapor Deposition Process, Chem. Phys. Lett. 367 (2003) 214 – 218.

[5] C. Oros, M. Horprathum, A. Wisitsoraat, T. Srichaiyaperk, B. Samransuksamer, S. Limwichean, P. Eiam-chai, D. Phokharatkul, N. Nuntawong, C. Chananonnawathorn, V. Patthanasettakul, A. Klamchuen, J. Kaewkhao, A. Tuantranont, P. Chindaudom, Ultrasensitive NO_2 sensor based on vertically aligned SnO_2 nanorods deposited by DC reactive magnetron sputtering with glancing angle deposition technique, Sens. Actuators B Chem. 223 (2016) 936 – 945.

[6] H. Du, J. Wang, Y. Sun, P. Yao, X. Li, N. Yu, Investigation of gas sensing properties of SnO_2/In_2O_3 composite hetero-nanofibers treated by oxygen plasma, Sens. Actuators B Chem. 206 (2015) 753 – 763.

[7] Y. Hou, A.H. Jayatissa, Enhancement of gas sensor response of nanocrystalline zinc oxide for ammonia by plasma treatment, Appl. Surf. Sci. 309 (2014) 46 – 53.

[8] A. Sharma, M. Tomar, V. Gupta, SnO_2 thin film sensor with enhanced response for NO_2 gas at lower temperatures, Sens. Actuators B Chem.156(2) (2011) 743 – 752.

[9] H.J. Gwon, H.G. Moon, H.W. Jang, S.J. Yoon, K.S. Yoo, Sensitivity enhancement of nanostructured SnO_2 gas sensors fabricated using the glancing angle deposition method, J. Nanosci. Nanotechnol. 13(4) (2013) 2740 – 2744.

[10] C. Zhang, J. Wang, X. Geng, Tungsten oxide coatings deposited by plasma spray using powder and solution precursor for detection of nitrogen dioxide gas, J. Alloys Compd. 668 (2016) 128 – 136.

[11] M.Z. Ahmada, A. Wisitsoraat, A.S. Zoolfakar, R.A. Kadir, W. Wlodarski, Investigation of RF sputtered tungsten trioxide nanorod thin film gas sensors prepared with a glancing angle deposition method toward reductive and oxidative analytes, Sens. Actuators B Chem.183 (2013) 364 – 371.

[12] M. Horprathum, T. Srichaiyaperk, B. Samransuksamer, A. Wisitsoraat, P. Eiamchai, S. Limwichean, C. Chananonnawathorn, K. Aiempanakit, N. Nuntawong, V. Patthanasettakul, C. Oros, S. Porntheeraphat, P. Songsiriritthigul, H. Nakajima, A. Tuantranont, P. Chindaudom, Ultrasensitive Hydrogen Sensor Based on Pt-Decorated WO_3 Nanorods Prepared by Glancing-Angle dc Magnetron Sputtering, ACS Appl. Mater. Interfaces. 6 (2014) 22051 – 22060.

[13] H.W. Kim, S.W. Choi, A. Katoch, S.S. Kim, Enhanced sensing performances of networked SnO_2 nanowires by surface modification with atmospheric pressure Ar–O_2 plasma, Sens. Actuators B Chem. 177 (2013) 654 – 658.

[14] Y.H. Liang, W. Jun, Z. Biao, Z.B. Wen, L.L. Qin, Z.Y. Wu, Z. Cheng, X.X. Ling, Fabrication of single crystalline WO_3 nano-belts based photoelectric gas sensor for detection of high concentration ethanol gas at room temperature, Sens. Actuator A Phys. 303 (2020) 11 – 18.

[15] K. Khojier, S. Zolghadr, F. Teimoori, S. Goudarzi, Fabrication and characterization of porous WO_3 thin film as a high accuracy cyclohexene sensor, Mater. Sci. Semicond. Process. 118 (2020) 115 – 220.

[16] M. O'Brien, K. Lee, R. Morrish, N. C. Berner, N. McEvoy, C. A. Wolden, G. S. Duesberg, Plasma assisted synthesis of WS_2 for gas sensing applications, Chem. Phys. Lett. 615 (2014) 6 – 10.

[17] Y. Zhang, J. Li, G. An, X. He, Highly porous SnO_2 fibers by electrospinning and oxygen plasma etching and its ethanol-sensing properties, Sens. Actuators B Chem. 44 (2010) 43 – 48.

[18] B. Urasinska-Wojcik, T.A. Vincent, J.W. Gardner, H_2S sensing properties of WO_3 based gas sensor, Procedia Engineering. 168 (2016) 255 – 258.

[19] M. Takácsa and A.E. Pap, Gas sensitivity of sol-gel prepared mesoporous WO_3 thin film, Procedia Engineering. 168 (2016) 289 – 292.

[20] T. Shujah, M. Ikram, A. R. Butt, M.K. Shahzad, K. Rashid, Q. Zafar, S. Ali, H_2S Gas Sensor Based on WO_3 Nanostructures Synthesized via Aerosol Assisted Chemical Vapor Deposition Technique, nanoscience and Nanotechnology Letters. 11 (2019) 1 – 10.